

***Supplementary Materials:***

**Fabrication dual-functional electrodes of oxygen vacancy abundant  
NiCo<sub>2</sub>O<sub>4</sub> nanosheets for advanced hybrid supercapacitors and Zn-ion  
batteries**

Jinhe Wei,<sup>a</sup> Jiaqing Guo,<sup>c</sup> Siyu Wang,<sup>a</sup> Ning Ding,<sup>a</sup> Pengcheng Xu,<sup>a</sup> Ping Wang,<sup>a</sup>  
Dandan Han,<sup>\*a</sup> Yen Wei <sup>\*b</sup> and Xiaohong Yin <sup>\*c</sup>

<sup>a</sup> *College of Chemistry and Pharmaceutical Engineering, Jilin Institute of Chemical  
Technology, Jilin 132022, China*

<sup>b</sup> *Department of Chemistry and the Tsinghua Center for Frontier Polymer Research,  
Tsinghua University, Beijing, 100084, China*

<sup>c</sup> *School of Chemistry and Chemical Engineering, Tianjin University of Technology,  
Tianjin 300384, China*

<sup>\*</sup>Corresponding author.

*E-mail address:* handandan@jlict.edu.cn (D.H.); weiyen@tsinghua.edu.cn (Y.W.);  
yinxiaohong@tjut.edu.cn (X.Y.)

### **Preparation of Co<sub>3</sub>O<sub>4</sub> nanosheets**

The electrodes of Co<sub>3</sub>O<sub>4</sub> and ZnCo<sub>2</sub>O<sub>4</sub> are synthesized using a similar method. For the preparation the Co<sub>3</sub>O<sub>4</sub> on Ni foam, the used 2.5 mmol Co(NO<sub>3</sub>)<sub>2</sub>·6H<sub>2</sub>O, 5 mmol of NH<sub>4</sub>F and 12.5 mmol C<sub>6</sub>H<sub>12</sub>N<sub>4</sub> were dissolved in a mixed solution of 30 mL of H<sub>2</sub>O stirring for 30 min. After that, the mixed solution was sealed and kept at 120 °C for 5 h. The Co<sub>3</sub>O<sub>4</sub> nanowires were obtained by calcination of the Co precursor at 350 °C for 2 h at a rate of 2 °C·min<sup>-1</sup>.

### **Preparation of ZnCo<sub>2</sub>O<sub>4</sub> nanosheets**

For the synthesis of ZnCo<sub>2</sub>O<sub>4</sub> on Ni foam, the used 1 mmol Zn(NO<sub>3</sub>)<sub>2</sub>·6H<sub>2</sub>O, 5 mmol Co(NO<sub>3</sub>)<sub>2</sub>·6H<sub>2</sub>O, 2 mmol of NH<sub>4</sub>F and 5 mmol C<sub>6</sub>H<sub>12</sub>N<sub>4</sub> were dissolved in a mixed solution of 40 mL of H<sub>2</sub>O stirring for 30 min. After that, the mixed solution was sealed and kept at 120 °C for 5 h. The ZnCo<sub>2</sub>O<sub>4</sub> nanowires were obtained by calcination of the Zn-Co precursor at 400 °C for 2 hours at a rate of 2 °C·min<sup>-1</sup>.

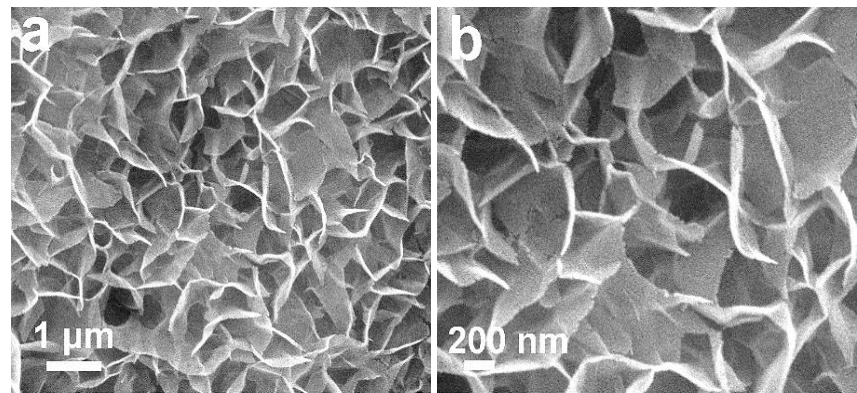


**Figure S1** (a, b) SEM image of the  $\text{NiCo}_2\text{O}_4$  samples.

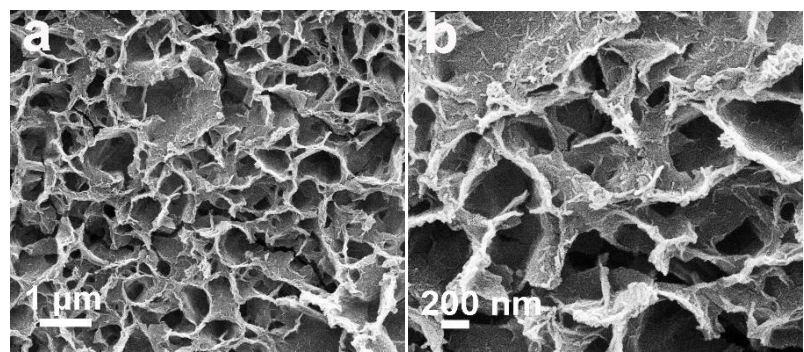


**Figure S2** (a, b) SEM image of the V-NiCo<sub>2</sub>O<sub>4</sub>-3 samples.

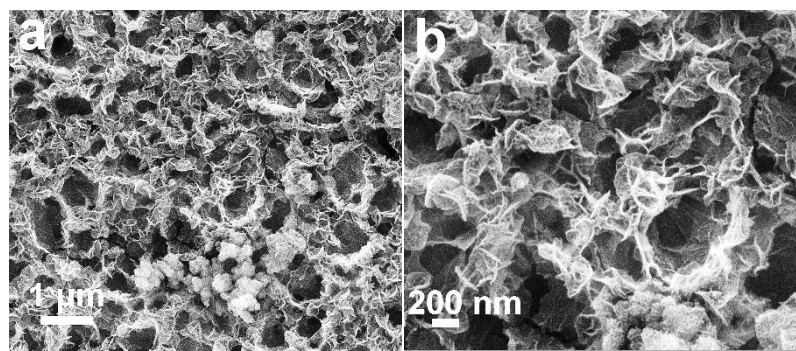


**Figure S3** (a, b) SEM image of the V-NiCo<sub>2</sub>O<sub>4</sub>-5 samples.

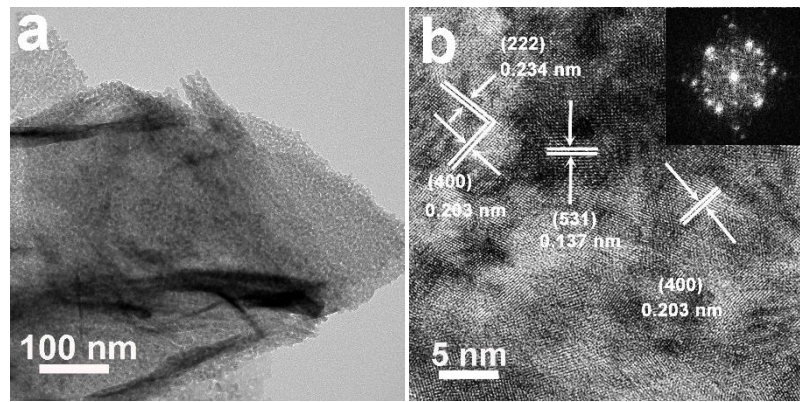


**Figure S4** TEM images and (d) high-resolution TEM image of  $\text{NiCo}_2\text{O}_4$ .

**Table S1** XPS peak area ratios of NiCo<sub>2</sub>O<sub>4</sub> and V-NiCo<sub>2</sub>O<sub>4</sub>-4.

Peak identity \ Materials	2P <sub>1/2</sub> Co <sup>2+</sup>	2P <sub>1/2</sub> Co <sup>3+</sup>	2P <sub>3/2</sub> Co <sup>2+</sup>	2P <sub>3/2</sub> Co <sup>3+</sup>	2P <sub>1/2</sub> Ni <sup>2+</sup>	2P <sub>1/2</sub> Ni <sup>3+</sup>	2P <sub>3/2</sub> Ni <sup>2+</sup>	2P <sub>3/2</sub> Ni <sup>3+</sup>	O <b>I</b>	O <b>II</b>	O <b>III</b>
NiCo <sub>2</sub> O <sub>4</sub>	0.48	0.52	0.53	0.47	0.43	0.57	0.60	0.40	0.26	0.37	0.42
V-NiCo <sub>2</sub> O <sub>4</sub> -4	0.63	0.37	0.68	0.32	0.52	0.48	0.63	0.37	0.32	0.55	0.13

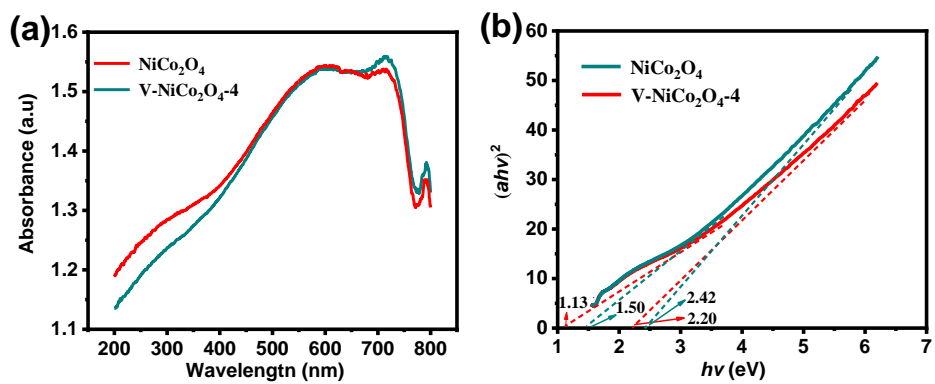


**Figure S5** (a) UV-vis absorbance spectra of  $\text{NiCo}_2\text{O}_4$  and  $\text{V-NiCo}_2\text{O}_4\text{-}4$  samples; (c) The experimental bandgaps of  $\text{NiCo}_2\text{O}_4$  and  $\text{V-NiCo}_2\text{O}_4\text{-}4$  samples.

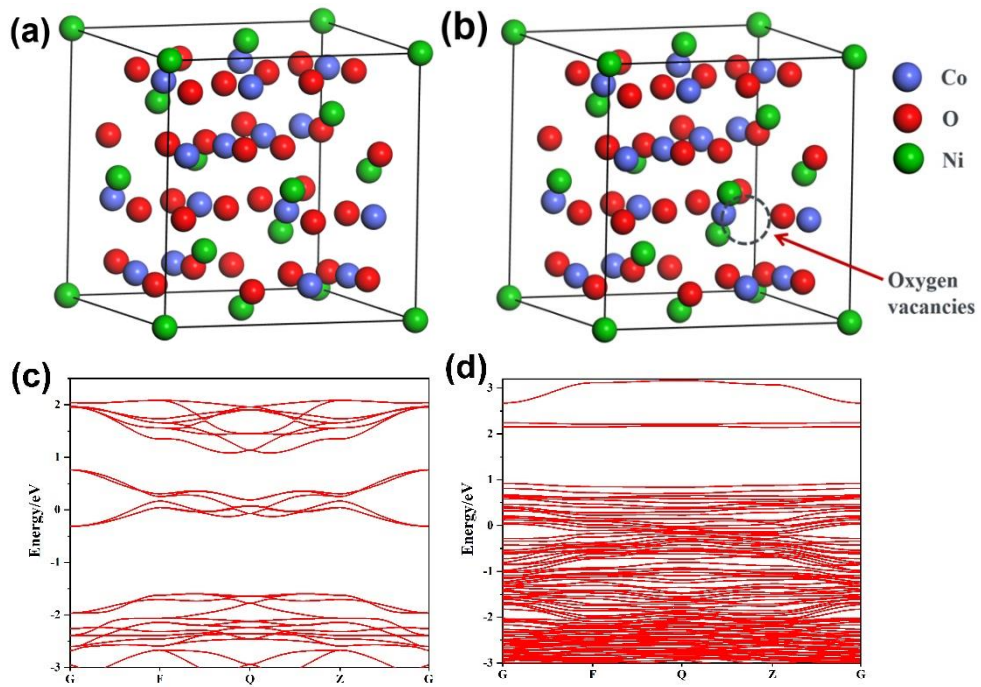


**Figure S6** The atomic structure of  $\text{NiCo}_2\text{O}_4$  (a) and  $\text{V-NiCo}_2\text{O}_4\text{-4}$  (b); Minority spin channel in  $\text{NiCo}_2\text{O}_4$  (c) and  $\text{V-NiCo}_2\text{O}_4\text{-4}$  (d).

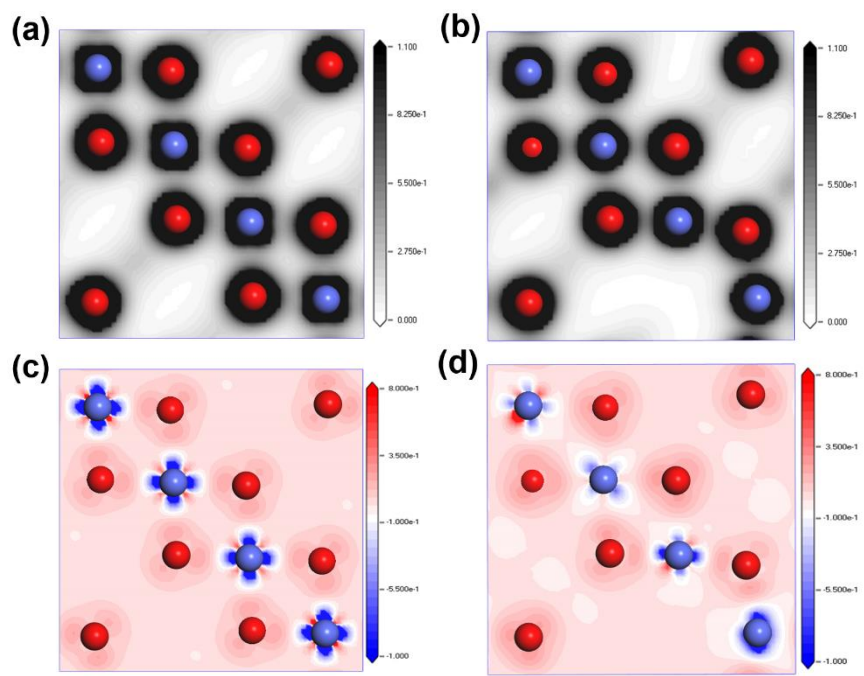


**Figure S7** (a, b) electrons density image of NiCo<sub>2</sub>O<sub>4</sub> and V-NiCo<sub>2</sub>O<sub>4</sub>-4; (c, d) electron density difference of NiCo<sub>2</sub>O<sub>4</sub> and V-NiCo<sub>2</sub>O<sub>4</sub>-4.

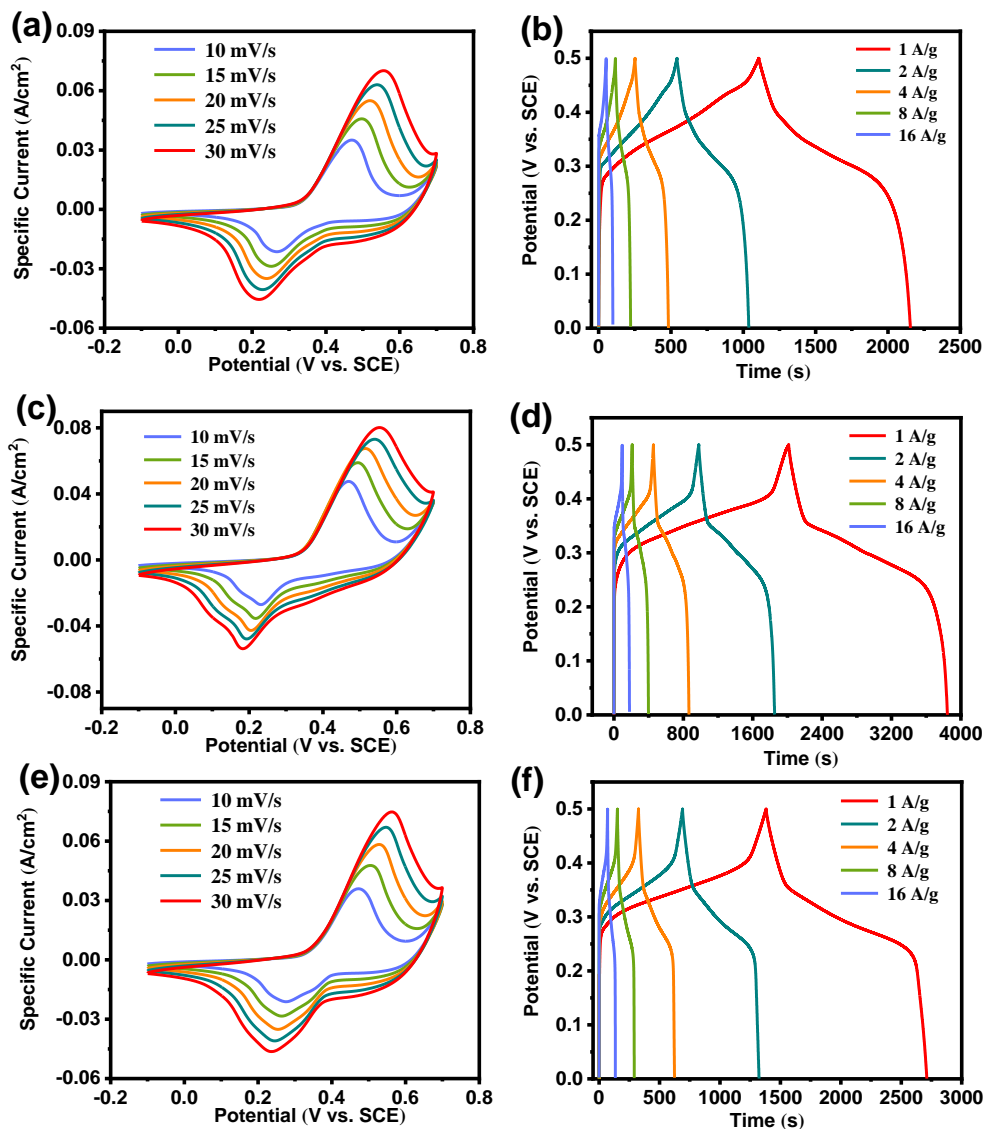


**Figure S8** (a, c, e) CV curves of  $\text{NiCo}_2\text{O}_4$ ,  $\text{V-NiCo}_2\text{O}_4\text{-3}$ ,  $\text{V-NiCo}_2\text{O}_4\text{-5}$  electrodes at different scan rates; (b, d, f) GCD curves of the  $\text{NiCo}_2\text{O}_4$ ,  $\text{V-NiCo}_2\text{O}_4\text{-3}$ ,  $\text{V-NiCo}_2\text{O}_4\text{-5}$  electrodes at different specific currents.

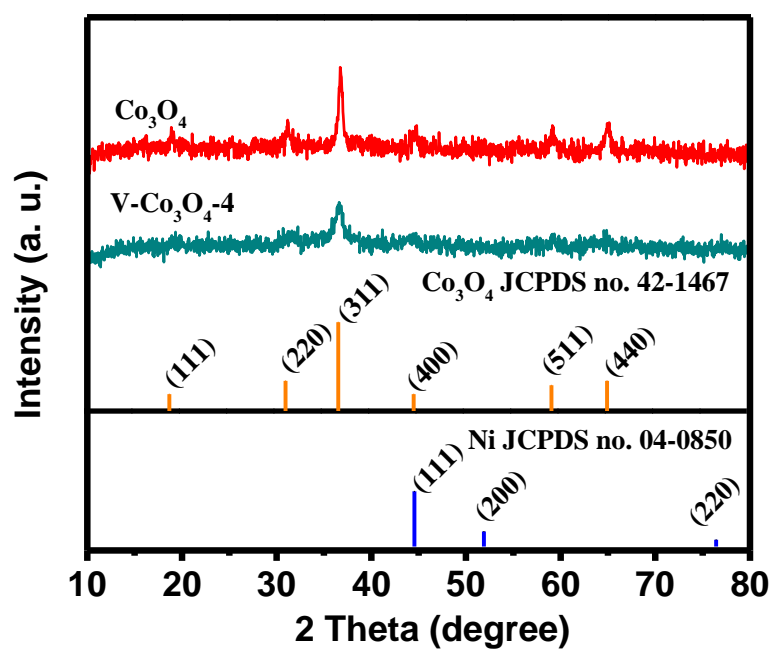


**Figure S9** XRD patterns of  $\text{Co}_3\text{O}_4$  and  $\text{Co}_3\text{O}_4\text{-}4$ .

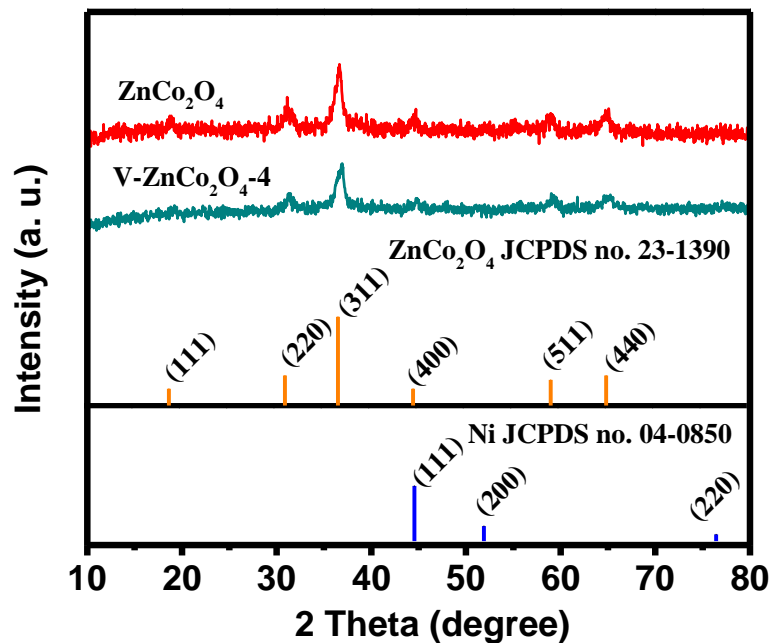


**Figure S10** XRD patterns of  $\text{ZnCo}_2\text{O}_4$  and  $\text{V-ZnCo}_2\text{O}_4\text{-}4$ .

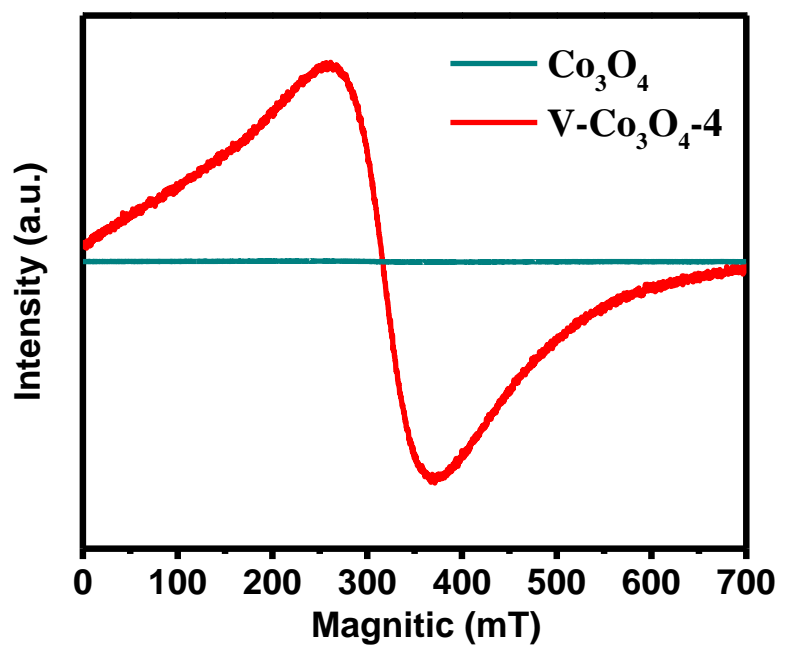


**Figure S11** EPR spectra of  $\text{Co}_3\text{O}_4$  and  $\text{Co}_3\text{O}_4-4$ .

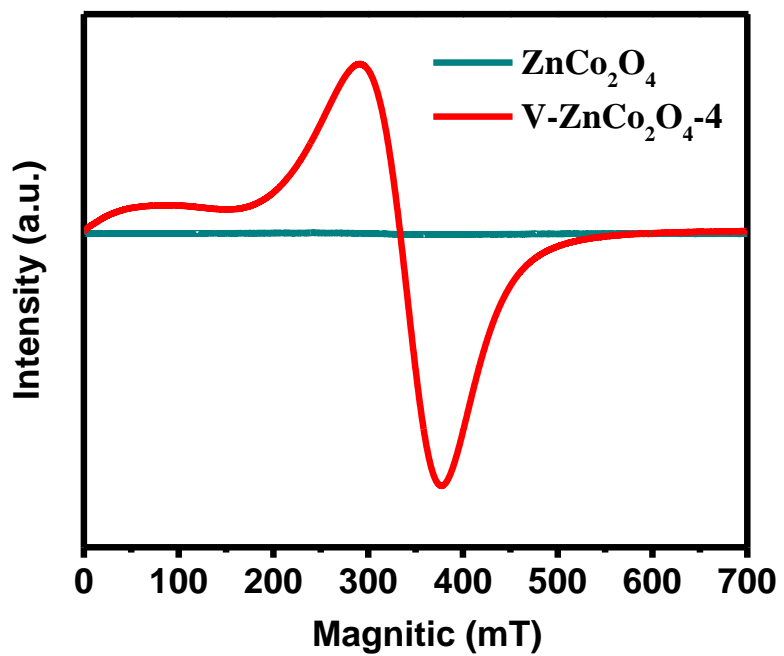
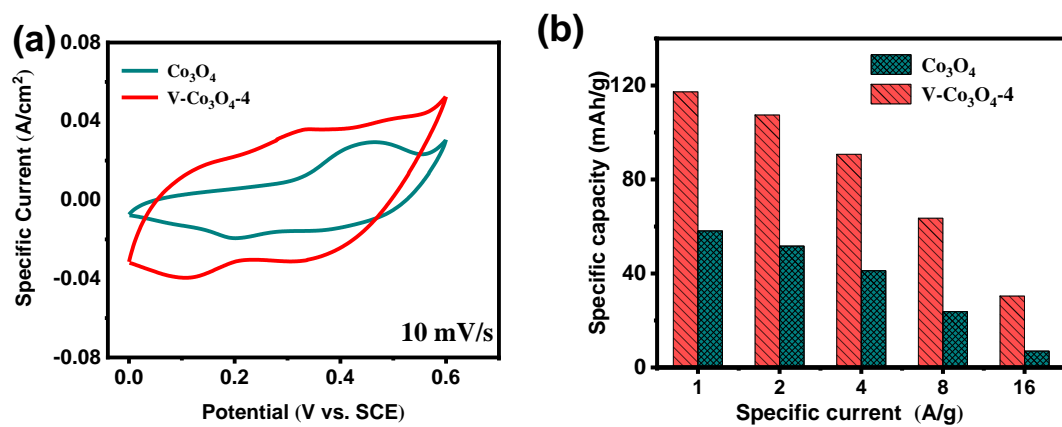


**Figure S12** EPR spectra of  $\text{ZnCo}_2\text{O}_4$  and  $\text{V-ZnCo}_2\text{O}_4\text{-}4$ .



**ure S13** (a) CV curves of  $\text{Co}_3\text{O}_4$  and  $\text{Co}_3\text{O}_4-4$  at the scan rate of  $10 \text{ mV}\cdot\text{s}^{-1}$ ; (b) Specific discharge capacitance at different current densities of  $\text{Co}_3\text{O}_4$  and  $\text{Co}_3\text{O}_4-4$  h.

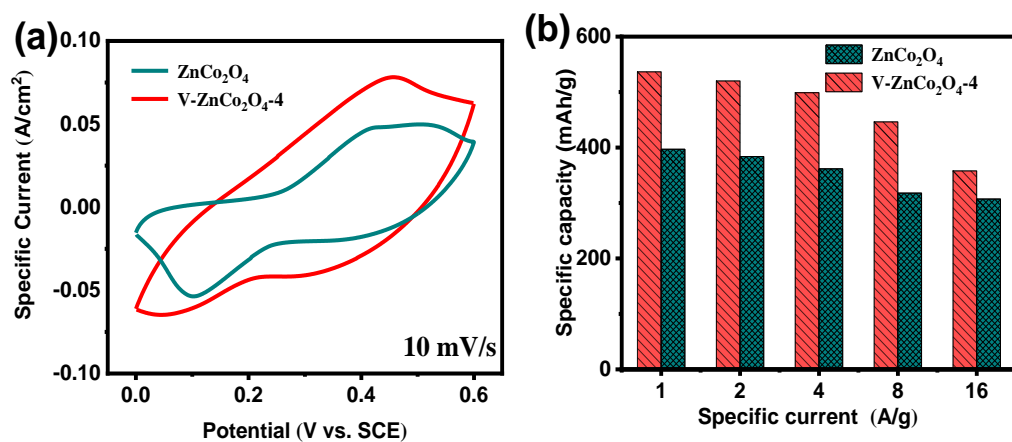


**Figure S14** (a) CV curves of  $\text{ZnCo}_2\text{O}_4$  and  $\text{V-ZnCo}_2\text{O}_4\text{-}4$  at the scan rate of  $10 \text{ mV}\cdot\text{s}^{-1}$ ; (b) Specific discharge capacitance at different current densities of  $\text{ZnCo}_2\text{O}_4$  and  $\text{V-ZnCo}_2\text{O}_4\text{-}4$ .

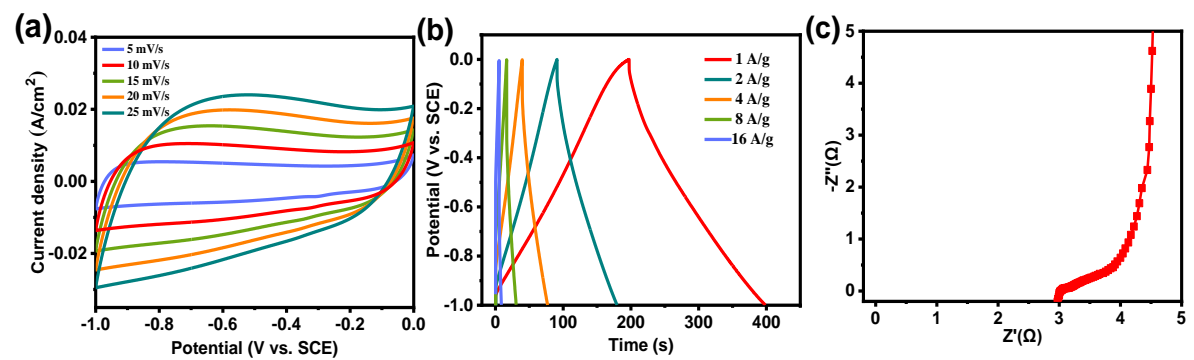


**Figure S15** (a) CV curves of AC; (b) GCD curves of AC; (c) EIS curve of AC.

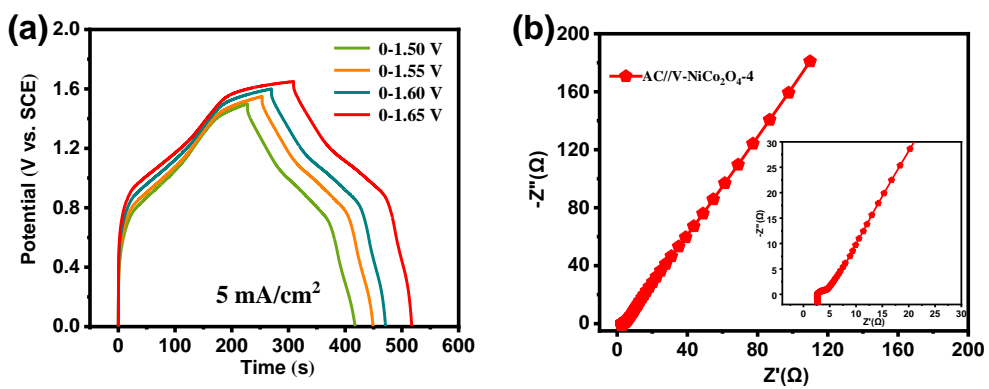


**Figure S16** (a) GCD curves of the V-NiCo<sub>2</sub>O<sub>4</sub>-4//AC HSC device at different voltages (from 1.5 to 1.8 V) at a specific current of 30 mA·cm<sup>-2</sup>; (b) EIS curves of the assembled V-NiCo<sub>2</sub>O<sub>4</sub>-4//AC HSC device.

**Table S2.** Comparison of the similar device properties of the oxygen-deficient metal oxide as cathode

Material	Electrolyte	Performance	Cycling stability of Device	Sr. No
L-CuCo <sub>2</sub> O <sub>4</sub>	3 M KOH	139.72 mAh·g <sup>-1</sup> at 1 A·g <sup>-1</sup>	85.5% after 10000 cycles	1
150-N:ZnCo <sub>2</sub> O <sub>4</sub>	3 M KOH	422.73 mAh·g <sup>-1</sup> at 5 A·g <sup>-1</sup>	95.4% after 3000 cycles	2
OV-MgCo <sub>2</sub> O <sub>4</sub>	3 M KOH	54.11 mAh·g <sup>-1</sup> at 1 A·g <sup>-1</sup>	82% after 10000 cycles	3
OV-ZnCo <sub>2</sub> O <sub>4</sub>	6 M KOH	293.14 mAh·g <sup>-1</sup> at 1 A·g <sup>-1</sup>	No cycling	4
ZnMoO <sub>4</sub> -OV	6 M KOH	209.12 mAh·g <sup>-1</sup> at 1.4 A·g <sup>-1</sup>	87.4% after 10000 cycles	5
P-NiMoO <sub>4</sub>	1 M KOH	142.88 mAh·g <sup>-1</sup> at 1.4 A·g <sup>-1</sup>	98.7% after 5000 cycles	6
N-Bi <sub>2</sub> MoO <sub>6</sub>	6 M KOH	155.13 mAh·g <sup>-1</sup> at 0.5 A·g <sup>-1</sup>	79% after 10000 cycles	7
Ov-NiMn-LDH	2 M KOH	32.8.6 mAh·g <sup>-1</sup> at 1 A·g <sup>-1</sup>	No cycling	8
Co <sub>3</sub> O <sub>4</sub> @Co/NC-HN	3 M KOH	273.9 mAh·g <sup>-1</sup> at 1 A·g <sup>-1</sup>	92.6% after 4000 cycles	9
v-Co <sub>3</sub> O <sub>4</sub> /CC	2 M LiOH	51.75 mAh·g <sup>-1</sup> at 1 A·g <sup>-1</sup>	81.4% after 5000 cycles	10
N-GNTs@OV-Bi <sub>2</sub> O <sub>3</sub>	6 M KOH	196.47 mAh·g <sup>-1</sup> at 1 A·g <sup>-1</sup>	85% after 10000 cycles	11
Vo-NiCo LDH	6 M KOH	217.1 mAh·g <sup>-1</sup> at 1 A·g <sup>-1</sup>	75% after 10000 cycles	12
MoO <sub>3-x</sub>	1 M H <sub>2</sub> SO <sub>4</sub>	273.33 mAh·g <sup>-1</sup> at 5 A·g <sup>-1</sup>	75% after 10000 cycles	13
Pd-Co <sub>3</sub> O <sub>4</sub>	6 M KOH	181.92 mAh·g <sup>-1</sup> at 2 .06 A·g <sup>-1</sup>	92.5% after 4000 cycles	14
L-CoFe <sub>2</sub> O <sub>4</sub> /C	2 M KOH	66.67 mAh·g <sup>-1</sup> at 1 A·g <sup>-1</sup>	No cycling	15
Ov-MnO <sub>2</sub> @MnO <sub>2</sub>	1 M Na <sub>2</sub> SO <sub>4</sub>	125.67 mAh·g <sup>-1</sup> at 1 A·g <sup>-1</sup>	82% after 10000 cycles	16
α-MnO <sub>2</sub>	1 M KOH	204.53 mAh·g <sup>-1</sup> at 1 A·g <sup>-1</sup>	80.6% after 10000 cycles	17
LOV-MnO <sub>2</sub>	1 M Na <sub>2</sub> SO <sub>4</sub>	126.42 mAh·g <sup>-1</sup> at 1 A·g <sup>-1</sup>	92.2% after 10000 cycles	18
<b>V-NiCo<sub>2</sub>O<sub>4</sub>-4</b>	<b>2 M KOH</b>	<b>751.67 mAh·g<sup>-1</sup> at 1 A·g<sup>-1</sup></b>	<b>91.9% after 10000 cycles</b>	<b>This work</b>

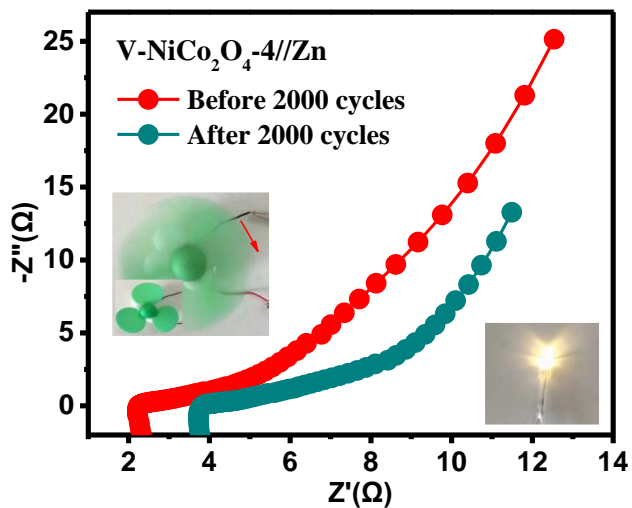


**Figure S17** EIS curves of the as-assembled V-NiCo<sub>2</sub>O<sub>4</sub>-4//Zn batteries.

## References

- [1] Y. M. Feng, W. F. Liu, Y. Wang, W. N. Gao, J. T. Li, K. L. Liu, X. P. Wang and J. Jiang, *J. Power Sources*, 2020, **458**, 228005.
- [2] I. K. Moon, S. Yoon, B. Ki, K. Choi and J. Oh, *ACS Appl. Energy Mater.*, 2018, 1, 4804-4813.
- [3] H. Z. Wang, N. Y. Mi, S. F. Sun, W. G. Zhang and S. W. Yao, *J. Alloys Compd.*, 2021, **869**, 159294.
- [4] K. Xiang, D. Wu, Y. Fan, W. You, D. D. Zhang, J. L. Luo and X. Z. Fu, *Chem. Eng. J.*, 2021, **425**, 130583.
- [5] P. X. Li, J. P. Wang, L. M. Li, S. L. Song, X. M. Yuan, W. Q. Jiao, Z. Hao and X. L. Li, *New J. Chem.*, 2021, **45**, 9026.
- [6] F. F. Wang, K. Ma, W. Tian, J. C. Dong, H. Han, H. P. Wang, K. Deng, H. R. Yue, Y. X. Zhang, W. Jiang and J. Y. Ji, *J. Mater. Chem. A*, 2019, **7**, 19589-19596.
- [7] T. Ma, S. M. Jin, X. D. Kong, M. Lv, H. Wang, X. Y. Luo, H. F. Tan, Z. W. Li, Y. Zhang, X. H. Chang and X. L. Song, *Appl. Surf. Sci.*, 2021, **548**, 149244.
- [8] Y. Q. Tang, H. M. Shen, J. Q. Cheng, Z. B. Liang, C. Qu, H. Tabassum and R. Q. Zou, *Adv. Funct. Mater.*, 2020, **30**, 1908223.
- [9] L. D. Wang, X. F. Li, S. S. Xiong, H. J. Lin, Y. C. Xu, Y. Jiao and J. R. Chen, *J. Colloid Interface Sci.*, 2021, **600**, 58-71.
- [10] S. Dai, F. F. Han, J. Tang and W. H. Tang, *Electrochim. Acta*, 2019, **328**, 135103.
- [11] J. Zhao, Z. Li, T. Shen, X. Yuan, G. Qiu, Q. Jiang, Y. Lin, G. song, A. Meng and Q. Li, *J. Mater. Chem. A*, 2019, **7**, 7918-7931.

- [12] H. Y. Liang, H. A. Jia, T. S. Lin, Z. Y. Wang, C. Li, S. L. Chen, J. L. Qi, J. Cao, W. D. Fei and J. C. Feng, *J. Colloid Interface Sci.*, 2019, **554**, 59-65.
- [13] Q. L. Wu, S. X. Zhao, L. Yu, X. X. Zheng, Y. F. Wang, L. Q. Yu, C. W. Nan and G. Z. Cao, *J. Mater. Chem. A*, 2019, **7**, 13205-13214.
- [14] J. X. Hao, S. L. Peng, H. Q. Li, S. Dang, T. F. Qin, Y. X. Wen, J. J. Huang, F. Ma, D. Q. Gao, F. Li and G. Z. Cao, *J. Mater. Chem. A*, 2018, **6**, 16094-16100.
- [15] Y. Zhao, Y. G. Xu, J. Zeng, B. Kong, X. W. Geng, D. W. Li, X. Gao, K. Liang, L. Xu, J. B. Lian, S. Q. Huang, J. X. Qiu, Y. P. Huang and H. M. Li, *RSC Adv.*, 2017, **7**, 55513-55522.
- [16] Y. S. Fu, X. Y. Gao, D. S. Zhang, J. W. Zhu, X. Ouyang and X. Wang, *J. Mater. Chem. A*, 2018, **6**, 1601-1611.
- [17] Y. C. Chen, C. B. Zhou, G. Liu, C. X. Kang, L. Ma and Q. M. Liu, *J. Mater. Chem. A*, 2021, **9**, 2872-2887.
- [18] P. Cui, Y. X. Zhang, Z. Cao, Y. P. Liu, Z. H. Sun, S. T. Cheng, Y. Wu, J. C. Fu and E. Q. Xie, *Chem. Eng. J.*, 2021, **412**, 128676.